Supporting Information

Dupuis et al. 10.1073/pnas.1316039111

SI Text

RNA Construct and Reagents

The model tetraloop–receptor RNA construct (Fig. 1) is assembled by annealing together three pieces of RNA that were purchased from IDT: (*i*) a DNA surface tether strand, 5′-biotin-CGC ACT CGT CTG AG-3′; (*ii*) a Cy3-labeled tetraloop-linker-helix strand, 5′-Cy3-GGC GAA AGC C-PEG$_6$-CGU GUC GUC CUA AGU CGG C-3′; and (*iii*) a Cy5-labeled helix strand, 5′-Cy5-GCC GAU AUG GAC GAC ACG CCC CUC AGA CGA GUG CG-3′. Sandwich-style sample holders were prepared by making a channel between a glass slide and a coverslip separated by two strips of double-sided tape. The channel is flushed with a 10:1 mixture of BSA:BSA-biotin at ∼1 mg/mL total protein concentration, followed by streptavidin (∼0.1 mg/mL) and lastly the tetraloop–receptor RNA construct at ∼100 pM dilution. Just before imaging, the channel is flushed with an imaging solution that contains the following: (*i*) 50 mM Hepes buffer (pH 7.5), (*ii*) 0–100 mM NaCl and 0.1 mM EDTH, (*iii*) 2 mM Trolox (9-hydroxy-2,5,7,8-tetramethylchroman-2-carboxylic acid), (*iv*) ∼0.1 mg/mL protocatechuate 3,4-dioxygenase (PCD), (*v*) ∼10 mM 3,4-dihydroxybenzoic acid (PCA) to catalytically remove oxygen, and (*vi*) PEG 8000 to achieve the desired solution conditions.

Confocal Imaging

Surface immobilized molecules are imaged with a home-built confocal microscope that has been described in detail elsewhere (1, 2). Briefly, the samples are illuminated with 532-nm light from a pulsed ND:YAG laser (10 ps at 20 MHz) that is focused to a diffraction limited spot by a 1.2 N.A. water immersion objective. The total fluorescence from single dye-labeled RNA molecules is collected through the same objective, focused through a 50-μm pinhole, and split into Cy3 and Cy5 channels with dichroics (645 nm) just before collection by avalanche photodiodes. Background correction, E_{FRET} calculation, and dwell time analysis are performed with in-house written software.

As in previous studies, the kinetics of GAAA tetraloop–receptor folding is measured from single-molecule fluorescence intensity trajectories as follows (2–8). Folding and unfolding events are observed as anticorrelated intensity fluctuations between the Cy3 and Cy5 channels. Fluorescence intensities are then used to calculate the fluorescence resonance energy transfer efficiency values (E_{FRET}), generating E_{FRET} trajectories, that reveal binary switching between high ($E_{FRET} \sim 0.7$) and low ($E_{FRET} \sim 0.3$) energy transfer efficiency (7). Crossings between high and low E_{FRET} define the time the construct spends in each state, or dwell times (τ_{fold} and τ_{unfold}), which are then integrated with cumulative distribution functions (CDFs) to describe the decay out of the folded and unfolded states (9). Under typical illumination intensities (1–2 μW), each individual molecule survives long enough to record between 5 and 50 switching events before irreversibly photobleaching. To build up the 200–500 total switching events to accurately describe the single-exponential decay out of each state, ∼10–50 individual molecules are monitored under one set of solution conditions. The aggregate switching events are then randomly sorted into three subdatasets and least-squares fit to single-exponential functions yielding unimolecular rate constants for folding (k_{fold}) and unfolding (k_{unfold}) (10, 11). The average and SD of the three independent fits are reported on the plots. Typically, the fractional error on individual data points is ∼10% of the absolute value.

To control the sample temperature for thermodynamic measurements, the sample is heated in two ways: (*i*) simultaneous proportional–integral–derivative controlled Peltier heating of both stage and objective and (*ii*) an IR laser tuned to the first overtone of the OH stretch of water (1,455 nm) and focused to a ∼17-μm spot coaxial with the visible laser excitation beam (7, 12). Both methods have been shown to provide temperature control to a precision and accuracy of ±0.1 °C (6–8, 12).

1. Hodak JH, Fiore JL, Nesbitt DJ, Downey CD, Pardi A (2005) Docking kinetics and equilibrium of a GAAA tetraloop-receptor motif probed by single-molecule FRET. *Proc Natl Acad Sci USA* 102(30):10505–10510.
2. Fiore JL, Hodak JH, Piestert O, Downey CD, Nesbitt DJ (2008) Monovalent and divalent promoted GAAA tetraloop-receptor tertiary interactions from freely diffusing single-molecule studies. *Biophys J* 95(8):3892–3905.
3. Downey CD, et al. (2006) Metal ion dependence, thermodynamics, and kinetics for intramolecular docking of a GAAA tetraloop and receptor connected by a flexible linker. *Biochemistry* 45(11):3664–3673.
4. Downey CD, Hodak J, Nesbitt D, Pardi A (2004) Structural dynamics of an RNA tertiary contact explored by single molecule fluorescence spectroscopy. *Biophys J* 86(1):189A–190A.
5. Fiore JL, Holmstrom ED, Fiegland LR, Hodak JH, Nesbitt DJ (2012) The role of counterion valence and size in GAAA tetraloop-receptor docking/undocking kinetics. *J Mol Biol* 423(2):198–216.
6. Fiore JL, Holmstrom ED, Nesbitt DJ (2012) Entropic origin of Mg^{2+}-facilitated RNA folding. *Proc Natl Acad Sci USA* 109(8):2902–2907.
7. Fiore JL, Kraemer B, Koberling F, Edmann R, Nesbitt DJ (2009) Enthalpy-driven RNA folding: Single-molecule thermodynamics of tetraloop-receptor tertiary interaction. *Biochemistry* 48(11):2550–2558.
8. Holmstrom ED, Fiore JL, Nesbitt DJ (2012) Thermodynamic origins of monovalent facilitated RNA folding. *Biochemistry* 51(18):3732–3743.
9. Blanco M, Walter NG (2010) Analysis of complex single-molecule FRET time trajectories. *Methods in Enzymology* 472:152–178.
10. Bartley LE, Zhuang XW, Das R, Chu S, Herschlag D (2003) Exploration of the transition state for tertiary structure formation between an RNA helix and a large structured RNA. *J Mol Biol* 328(5):1011–1026.
11. Zhou YJ, Zhuang XW (2006) Robust reconstruction of the rate constant distribution using the phase function method. *Biophys J* 91(11):4045–4053.
12. Holmstrom ED, Nesbitt DJ (2010) Real-time infrared overtone laser control of temperature in picoliter H_2O samples: "Nanobathtubs" for single molecule microscopy. *J Phys Chem Lett* 1(15):2264–2268.

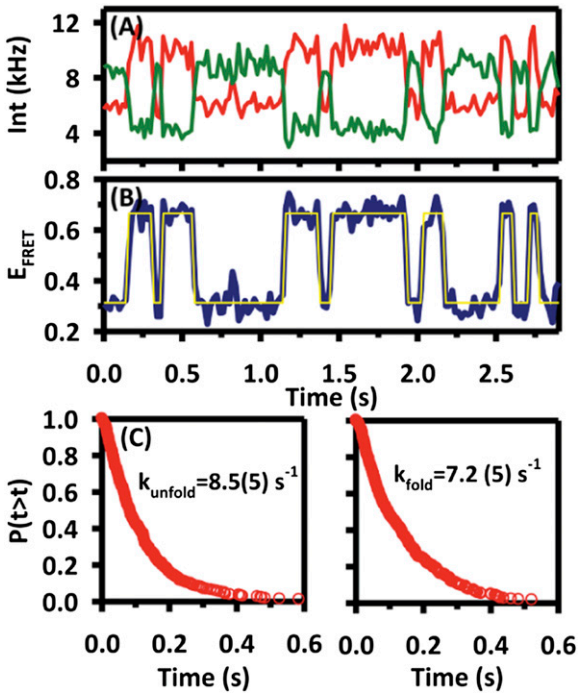

Fig. S1. Sample data analysis is shown. (*A*) Cy3 and Cy5 fluorescence time trajectories illustrate the anticorrelated intensity fluctuations due to folding and unfolding transitions. (*B*) The E_{FRET} time trajectory is calculated from fluorescence intensities revealing the binary two-state switching behavior. (*C*) The dwell times in the folded and unfolded states are used to construct the CDFs for folding and unfolding, which are then fit with single-exponential functions to extract k_{fold} and k_{unfold}.

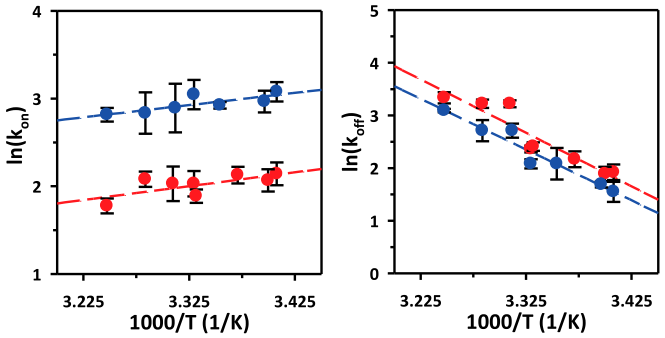

Fig. S2. Temperature dependences of the measured rate constants are shown in aqueous (red) and 8% PEG 8000 (blue) solutions. In both the folding (k_{on}) and unfolding (k_{off}) processes, the lines are parallel, indicating no significant change in the transition state enthalpies for either process. The largest effect is the upward offset of ln(k_{on}) under crowded conditions. Similar to our analysis of the equilibrium results, this uniform upward shift in k_{on} corresponds to crowding-induced changes in the entropy rather than enthalpy. However, with both forward and backward single-molecule rate constants explicitly measured as a function of temperature, the data further reveal that this shift arises predominantly from a reduction in the entropic cost of forming the transition state from the unfolded rather than folded state.